Electronic Band Structure Study of the Transport Properties of the Intermetallic Compounds ZrRuP and ZrRuSi

Dong-Kyun Seo, Jingqing Ren, and Myung-Hwan Whangbo*

Department of Chemistry, North Carolina State University, Raleigh, North Carolina 27695-8204

Enric Canadell

Institut de Ciencia de Materials de Barcelona (CSIC), 08193 Campus de la UAB, Bellaterra, Spain

Received February 7, 1997[⊗]

Electrical properties of the intermetallic superconductors h-ZrRuP, o-ZrRuP, and h-ZrRuSi were examined by calculating their electronic structures on the basis of the extended Hückel tight-binding method. To a first approximation, the electronic structure of ZrRuP is well described in terms of the oxidation state $Zr^{4+}(RuP)^{4-}$. This picture provides simple explanations for why both h-ZrRuP and o-ZrRuP have low $N(E_f)$ values and why h-ZrRuP has a nearly half-filled one-dimensional (1D) band dispersive along the *c* direction. A charge density wave instability associated with such a 1D band probably causes a *c*-axis doubling structural distortion in h-HfRuAs and h-TiRuAs. We discussed probable reasons for why the intermetallic phases with the *c*-axis doubling distortion are not superconductors and why h-ZrRuP has a higher T_c than does o-ZrRuP.

1. Introduction

Since the discovery of superconductivity in the intermetallic compound ZrRuP,[1] a number of studies have been carried out for ZrRuP and its analogs TT′X (T = Ti, Zr, Hf; T′ = Ru, Os; X = P, As).[2−9] Three different structural types are known for these compounds, i.e., the Fe_2P-type hexagonal structure (h-TT′X), the Co_2P-type orthorhombic structure (o-TT′X), and the TiFeSi-type orthorhombic structure (o′-TT′X). The o′-TT′X phase is closely related in structure to the h-TT′X phase; namely, it is a "dimerized" form of h-TT′X (see section 2). These intermetallic compounds exhibit interesting superconducting trends. Superconductivity is found only for the h-TT′X and o-TT′X phases, and the superconducting transition temperature T_c is generally higher for h-TT′X than for o-TT′X (e.g., 13.0 and 3.5 K for h-ZrRuP and o-ZrRuP, respectively).[5] Specific heat measurements for ZrRuP show that the Debye temperature Θ_D, which is a measure of the lattice stiffness, is lower for h-ZrRuP than for o-ZrRuP (345 versus 454 K).[8] According to the BCS mechanism of superconductivity,[10,11] this implies that the electron−phonon coupling constant λ is larger for h-ZrRuP (see section 5). Specific heat measurements reveal[3] that the numbers of electronic states at the Fermi level E_f, i.e., $N(E_f)$, are low for h-ZrRuP and h-HfRuP [i.e., 0.76 and 0.74 state/(eV·atom), respectively]. The high-temperature phase of HfRuAs (i.e., h-HfRuAs) is isostructural with h-ZrRuP and undergoes a structural phase transition near 1000 °C to o′-HfRuAs as the temperature is lowered.[6] h-HfRuAs, obtained by quenching to room temperature, exhibits superconductivity at 4.37−4.93 K, whereas o′-HfRuAs is not a superconductor down to 1 K.[6] The hexagonal phase of ZrRuSi is isostructural with h-TT′X.[12] An early study reported that h-ZrRuSi is not superconducting above 1.2 K.[1] In a recent study, however, Shirotani et al.[13] reported the preparation of an orthorhombic phase of ZrRuSi and their observation that both h-ZrRuSi and o-ZrRuSi phases are superconductors with higher T_c for the hexagonal phase as in the case of ZrRuP (i.e., 7−12 and 3−5 K for h-ZrRuSi and o-ZrRuSi, respectively). This similarity between ZrRuP and ZrRuSi is rather striking, since they are not isoelectronic. These observations lead to three important questions: Are there any structural and electronic reasons for why the $N(E_f)$ values of h-ZrRuP and h-HfRuP are low, why h-TT′X phases have a higher T_c than do o-TT′X phases, and why o′-TT′X phases do not show superconductivity?

In general, the orbitals around the highest occupied and the lowest unoccupied orbitals of "metal-rich" transition metal compounds are difficult to predict. For it is not straightforward how to describe the electronic structures of metal-rich compounds in terms of simple bonding concepts (e.g., symmetry, overlap, electronegativity, etc.). The structural change from h-HfRuAs to o′-HfRuAs amounts to a dimerization along the crystallographic *c* direction (see section 2). According to the concept of charge density wave (CDW) instability,[14−16] this suggests that h-HfRuAs has a half-filled one-dimensional (1D) band dispersive along the *c* direction. It is important to verify

[⊗] Abstract published in *Advance ACS Abstracts,* December 1, 1997.

(1) Barz, H.; Ku, H. C.; Meisner, G. P.; Fisk, Z.; Matthias, B. T. *Proc. Natl. Acad. Sci. U.S.A.* **1980**, *77*, 3132.
(2) Meisner, G. P.; Ku, H. C. In *Ternary Superconductors*; Shenoy, G. K., Dunlap, B. D., Fradin, F. Y., Eds.; North Holland, New York, 1981; p 255.
(3) Stewart, G. R.; Meisner, G. P.; Ku, H. C. In *Superconductivity in d- and f-band metals*; Buckel, W., Weber, W., Eds.; Kernforschungszentrum: Karlsruhe, Germany, 1982; p 331.
(4) Meisner, G. P.; Ku, H. C.; Barz, H. *Mater. Res. Bull.* **1983**, *18*, 983.
(5) Meisner, G. P.; Ku, H. C. *Appl. Phys.* **1983**, *31*, 201.
(6) Meisner, G. P. *Phys. Lett.* **1983**, *96*, 483.
(7) Müller, R.; Shelton, R. N.; Richardson, J. W., Jr.; Jacobson, R. A. *J. Less-Common Met.* **1983**, *92*, 177.
(8) Keiber, H.; Wühl, H.; Meisner, G. P.; Stewart, G. R. *J. Low Temp. Phys.* **1984**, *55*, 11.
(9) Shirotani, I.; Tachi, K.; Ichihashi, N.; Adachi, T.; Kikegawa, T.; Shimomura, O. *Phys. Lett. A* **1995**, *205*, 77.
(10) Bardeen, J.; Cooper, L. N.; Schrieffer, J. R. *Phys. Rev.* **1957**, *108*, 1175.
(11) McMillan, W. L. *Phys. Rev.* **1968**, *167*, 331.
(12) Johnson, V.; Jeitsschko, W. *J. Solid State Chem.* **1972**, *4*, 123.
(13) Shirotani, I.; Tachi, K.; Takeda, K.; Todo, S.; Yagi, T.; Kanoda, K. *Phys. Rev. B* **1995**, *52*, 6197.
(14) Whangbo, M.-H.; Canadell, E.; Foury, P.; Pouget, J.-P. *Science* **1991**, *252*, 96.
(15) Canadell, E.; Whangbo, M.-H. *Chem. Rev.* **1991**, *91*, 965.
(16) Whangbo, M.-H.; Canadell, E. *J. Am. Chem. Soc.* **1992**, *114*, 9587.

S0020-1669(97)00148-1 CCC: $14.00

Table 1. Exponents ζ_i and Valence-Shell Ionization Potentials H_{ii} of Slater-Type Orbitals χ_i Used for Extended Hückel Tight-Binding Calculations[a]

atom	χ_i	H_{ii} (eV)	ζ_i	c_1[b]	ζ_i'	c_2[b]
Zr	5s	−8.00	1.817			
Zr	5p	−5.40	1.776			
Zr	4d	−10.2	3.835	0.6224	1.505	0.5782
Ru	5s	−10.4	2.08			
Ru	5p	−6.87	2.04			
Ru	4d	−14.9	5.38	0.5342	2.300	0.6368
P	3s	−18.6	1.75			
P	3p	−14.0	1.30			
Si	3s	−17.3	1.383			
Si	3p	−9.20	1.383			

[a] H_{ii}'s are the diagonal matrix elements $\langle\chi_i|H^{\text{eff}}|\chi_i\rangle$, where H^{eff} is the effective Hamiltonian. In our calculations of the off-diagonal matrix elements $H^{\text{eff}} = \langle\chi_i|H^{\text{eff}}|\chi_j\rangle$, the weighted formula was used (Ammeter, J.; Bürgi, H.-B.; Thibeault, J.; Hoffmann, R. *J. Am. Chem. Soc*. **1978**, *100*, 3686). [b] Contraction coefficients used in the double-ζ Slater-type orbital.

if this is indeed the case and, if so, to see whether the occurrence of such a band can be understood in terms of the crystal structure and simple chemical bonding concepts.

In an effort to probe the questions discussed above, we analyze the crystal structures of h-ZrRuP, o-ZrRuP, and h-ZrRuSi and calculate their electronic band structures using the extended Hückel tight-binding method.[17] Calculations for o-ZrRuSi were not carried out because its structural data were not reported.[13] So far, no electronic band structure study has been reported for these compounds, although Miller and Cheng[18] recently examined the relative stabilities of several structural types of ZrNbP. The atomic parameters employed for our calculations are listed in Table 1.

2. Crystal Structures

To facilitate our discussion of the electronic structures of h-TT′X, o-TT′X, and o′-TT′X, we describe their crystal structures briefly. Structural building blocks common to h-TT′X and o-TT′X are −(T−T′)− zigzag chains **1a** along the crystallographic *c*-axis. A projection view of **1a** on the *ab* plane can be represented by **1b**.

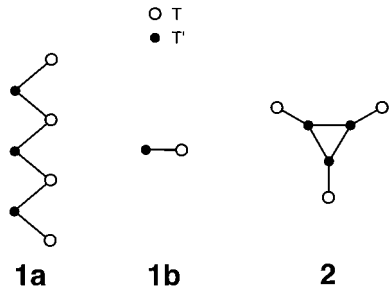

In the h-TT′X phase, every three −(T−T′)− chains form a −(T−T′)$_3$− triple chain **2** with formula $T_3T'_3$, in which the T′ atoms make a stack of T'_3 triangles along the *c*-axis such that the plane of each −(T−T′)− zigzag chain bisects the T'_3 triangles. An X atom site, i.e., X(2), is located at the center of each T'_6 trigonal prism formed with two adjacent T'_3 triangles (see **6a**). This leads to $T_3T'_3X(2)$ chains. In the 3D lattice **3** of h-TT'X, the $T_3T'_3X(2)$ chains are closely packed together, so that each T atom caps one rectangular face of an adjacent T'_6 trigonal prism and each T′ atom caps one rectangular face of an adjacent T_6 trigonal prism. The close packing results in two additional X atom sites, i.e., X(1), in a unit cell, each of

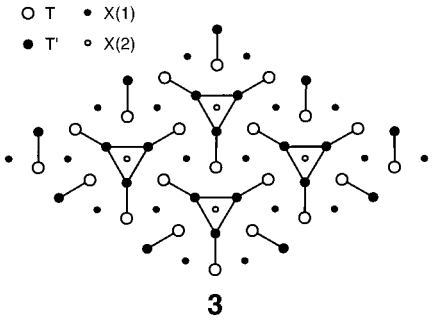

which is located at the center of a T_6 trigonal prism formed with two adjacent T_3 triangles. Thus a repeat unit of h-ZrRuP is given by $Zr_3Ru_3P(1)_2P(2)$. It is worth noting that h-ZrRuP consists of two kinds of prismatic chains, i.e., $P(1)Zr_3$ and $P(2)Ru_3$, running along the *c* direction.

In the o-TT′X phase,[7] every two −(T−T′)− chains form a −(T−T′)$_2$− double chain **4**, in which the T′ atoms make a −T′−T′− zigzag chain along the *c*-axis. These −(T−T′)$_2$− double

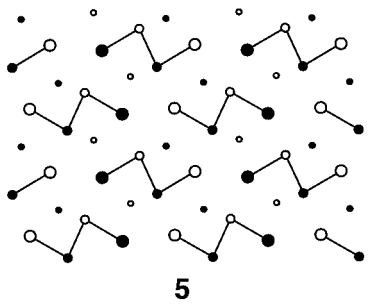

chains are closely packed to form a 3D lattice as shown in **5**, in which each X is located in the middle of a $T_4T'_2$ trigonal prism and all X sites are equivalent. Thus, o-ZrRuP consists of PZr_2Ru prismatic chains running along the *c* direction, and its unit cell is given by $Zr_4Ru_4P_4$.

The o′-TT′X phase is closely related in structure to h-TT′X. In h-TT′X all T'_3 triangles of each triple chain are parallel to the *ab* plane (**6a**). The o′-TT′X phase is derived from h-TT′X

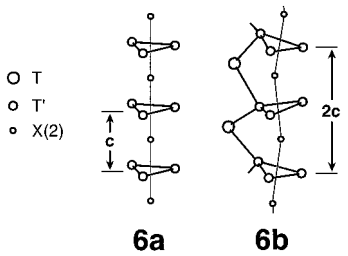

when all adjacent T'_3 triangles of each $X(2)T'_3$ prismatic chain are tilted in opposite directions (**6b**). The phase transition from h-TT′X to o′-TT′X does not strongly affect the $X(1)T_3$ prismatic chains. The structural change from **6a** to **6b** doubles the *c*-axis length. As already mentioned, this suggests that the h-TT′X phase has a half-filled 1D band dispersive along the *c* direction. Furthermore, this band should be largely associated with the $X(2)T'_3$ prismatic chains because the structures of the $X(1)T_3$ prismatic chains are only weakly modified by the h-TT′X to o′-TT′X phase transition. The o′-TT′X structure is found for the low-temperature phases of HfRuAs and TiRuAs[5] but is not found for ZrRuP.

(17) Whangbo, M.-H.; Hoffmann, R. *J. Am. Chem. Soc*. **1978**, *100*, 6093.
(18) Miller, G. J.; Cheng, J. *Inorg. Chem*. **1995**, *34*, 2962.

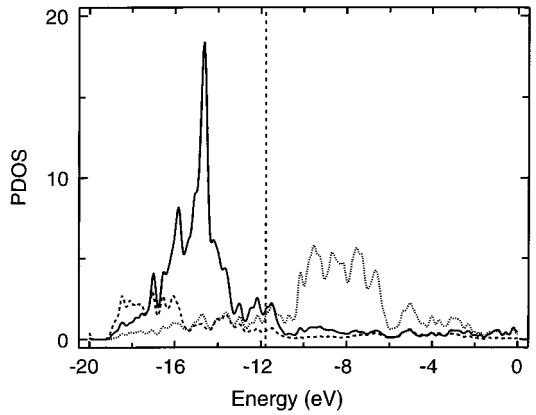

Figure 1. PDOS plots calculated for the Zr, Ru, and P atoms of h-ZrRuP. The solid, dotted, and dashed lines refer to the Ru, Zr, and P atoms, respectively.

3. Oxidation State of ZrRuP and Cause for Low $N(E_f)$ Values

Figure 1 shows contributions of the Zr, Ru, and P atoms to the total density of states (DOS), i.e., the projected density of states (PDOS), calculated for h-ZrRuP. Major contributions of Ru and P occur below E_f, and those of Zr, above E_f. In the occupied region, small contributions of Zr occur almost evenly, and in the region between the major peaks of Ru and Zr, the contributions of Zr, Ru, and P are small. To a first approximation, therefore, the bonding of ZrRuP can be described in terms of the oxidation state $Zr^{4+}(RuP)^{4-}$; i.e., the energy levels of ZrRuP can be approximated as a consequence of interactions between the empty d orbitals of Zr^{4+} and the occupied orbitals of $(RuP)^{4-}$. The oxidation state $(RuP)^{4-}$ can be rewritten as $(Ru^{2-})(P^{2-})$ or $(Ru^{-})(P^{3-})$, which implies that the d orbitals of Ru and the p orbitals of P are almost completely filled. Then the orbital interaction picture[19] predicts that the overlap populations for the Zr−Ru and Zr−P bonds are positive while those for the Ru−Ru and Ru−P bonds are negative around the Fermi level. Figure 2 presents plots of the crystal orbital overlap populations (COOP)[20] calculated for h-ZrRuP. In agreement with the prediction, the Zr−P contacts are bonding in all filled levels, and the Zr−Ru contacts in nearly all filled levels. The Ru−P(2) contact is bonding in nearly all filled levels, but the Ru−P(1) and Ru−Ru contacts are antibonding in a wide region of occupied levels (within ∼2.5 eV from E_f). This supports the bonding picture that the energy levels of h-ZrRuP can be viewed as a consequence of interactions between the empty d orbitals of Zr^{4+} and the occupied orbitals of $(RuP)^{4-}$.

An important consequence of the bonding picture for h-ZrRuP is that the Fermi level lies in the region of the states between the empty orbitals of Zr^{4+} and the filled orbitals of $(RuP)^{4-}$. As a result, the Fermi level occurs in the region where the DOS is low, so that the $N(E_f)$ value is calculated to be small [i.e., 0.21 state/(eV·atom)] in good agreement with experiment.[3]

The bonding picture based on the oxidation state $Zr^{4+}(RuP)^{4-}$ is also applicable to o-ZrRuP. Figure 3 shows the PDOS plots calculated for o-ZrRuP. In general, the PDOS plots of o-ZrRuP are similar to those of h-ZrRuP. However, the major contributions of Zr and Ru are spread over a wider region of energy in o-ZrRuP, which means stronger interactions between Zr and Ru in o-ZrRuP than in h-ZrRuP. This reflects the fact that the Zr−Ru distances are shorter in o-ZrRuP (2.903, 2 × 2.926, 2.967, 2 × 2.982 Å) than in h-ZrRuP (2 × 2.95, 4 × 3.00 Å). The Fermi level E_f of o-ZrRuP occurs where the DOS is low.

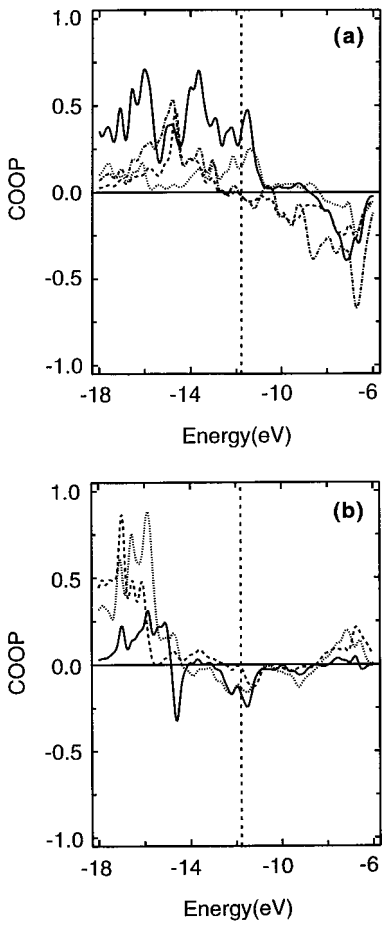

Figure 2. COOP plots calculated for a number of short interatomic contacts in h-ZrRuP: (a) Zr−P(1) (solid line), Zr−P(2) (dotted line), Zr−Ru within a triple chain **3** (dashed line), and Zr−Ru between triple chains (dashed−dotted line); (b) Ru−Ru (solid line), Ru−P(1) (dotted line), and Ru−P(2) (dashed line).

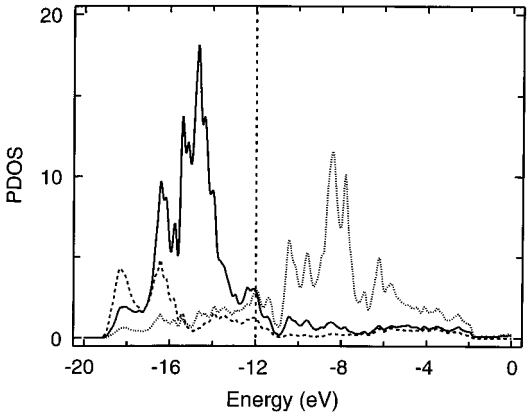

Figure 3. PDOS plots calculated for the Zr, Ru, and P atoms of o-ZrRuP. The solid, dotted, and dashed lines refer to the Ru, Zr, and P atoms, respectively.

The $N(E_f)$ value of o-ZrRuP, 0.29 state/(eV·atom), is small but is slightly larger than that of h-ZrRuP.

In a similar manner, the electronic structure of h-ZrRuSi may be described from the viewpoint of the oxidation state $Zr^{4+}(RuSi)^{4-}$. The PDOS plots calculated for h-ZrRuSi (Figure 4) are indeed consistent with this view. The major Ru peak is much sharper and major contributions of Zr are spread in a wider energy region for h-ZrRuSi than for h-ZrRuP. The major PDOS peak of Ru is narrow for h-ZrRuSi because the Ru−Ru distance is considerably longer in h-ZrRuSi than in h-ZrRuP (2.87 versus 2.63 Å). The $N(E_f)$ value of h-ZrRuSi, 0.39 state/(eV·atom), is small but is larger than that of h-ZrRuP.

(19) Albright, T. A.; Burdett, J. K.; Whangbo, M.-H. *Orbital Interactions in Chemistry*; Wiley: New York, 1985.
(20) Hughbanks, T.; Hoffmann, R. *J. Am. Chem. Soc.* **1983**, *105*, 3528.

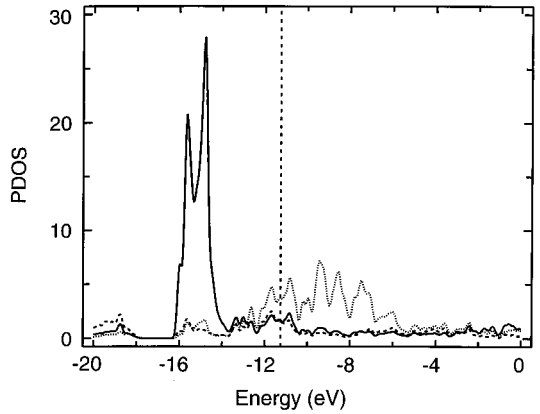

Figure 4. PDOS plots calculated for the Zr, Ru, and Si atoms of h-ZrRuSi. The solid, dotted, and dashed lines refer to the Ru, Zr, and Si atoms, respectively.

4. Half-Filled 1D Band and CDW Instability

In this section, a probable cause for the phase transition from h-TT′X to o′-TT′X in HfRuAs is examined in terms of the electronic structure calculated for h-ZrRuP. This approximation is reasonable because h-ZrRuP is isostructural and isoelectronic with h-HfRuAs. For our discussion, it is necessary to examine the band dispersion relations and Fermi surfaces of h-ZrRuP.

Figure 5a shows dispersion relations of the bands of h-ZrRuP in the vicinity of the Fermi level. There occur three partially-filled bands along the direction Γ−Z, two of which are degenerate. The Fermi surfaces associated with these bands are presented in Figure 5b as a cross-section view of the *YZ* plane and in Figure 5c as a perspective stereoview. To see the topological aspect of the Fermi surfaces, it is convenient to neglect the avoided crossings between Fermi surface sheets, as in the discussion of hidden Fermi surface nesting.[14−16] Then, one Fermi surface has the shape of a truncated cylinder along the *c*-axis and centered at Z. Another Fermi surface is nearly spherical in shape and is centered at Γ. The third Fermi surface consists of two warped 1D sheets. The 1D sheets are approximately nested by the vector $\sim c^*/2$; i.e., the 1D band is nearly half-filled (hereafter this band will be referred to as the half-filled 1D band).

The presence of the half-filled 1D band suggests a CDW instability leading to a *c*-axis doubling structural distortion. To explore this implication further, it is necessary to find the orbital character of this band. According to the crystal structure of h-ZrRuP (see **3** and **6a**), the orbitals that can have strong interactions only along the *c* direction are the P(1) $3p_z$ and Zr $4d_{z^2}$ orbitals of the P(1)Zr_3 prismatic chains and the P(2) $3p_z$ and Ru $4d_{z^2}$ orbitals of the P(2)Ru_3 prismatic chains. (The $4d_{xz}$ and $4d_{yz}$ orbitals of Zr and Ru give rise to strong interactions along the *c* direction as well as in the *ab* plane.) To determine the orbital character of the half-filled 1D band, PDOS plots were calculated for the $3p_z$ and $4d_{z^2}$ orbitals (Figure 6). In the energy region where the 1D band appears (i.e., between −14 and −11 eV in Figure 5a), contributions from the P(2) $3p_z$ and Ru $4d_{z^2}$ orbitals are both substantial, but this is not the case for the P(1) $3p_z$ and Zr $4d_{z^2}$ orbitals. Thus the half-filled 1D band is mainly associated with the P(2)Ru_3 prismatic chains. This finding is consistent with the $Zr^{4+}(RuP)^{4-}$ picture, because the P(1) $3p_z$ orbitals of the P(1)Zr_3 prismatic chains will be lowered in energy by the Zr $4d_{z^2}$ orbitals so that contributions of the P(1) $3p_z$ and Zr $4d_{z^2}$ orbitals are not strong in the region of the Fermi level.

As discussed above, h-ZrRuP has a half-filled 1D band dispersive along the *c* direction, and this band is largely associated with the P(2)Ru_3 prismatic chains. Thus the 1D band can cause a CDW instability leading to a *c*-axis doubling distortion in the P(2)Ru_3 prismatic chains (e.g., from **6a** to **6b**), thus giving rise to an o′-TT′X phase. However, for a metallic system with nested a Fermi surface to undergo a CDW transition, the electronic energy gain associated with it should be greater than the destabilization caused by the resulting lattice strain.[21] The fact that the "dimerized" o′-TT′X structure is found for HfRuAs and TiRuAs but not for ZrRuP suggests that the X(2)T'_3 prismatic chains are softer in "h-HfRuAs" and "TiRuAs" than in h-ZrRuP. The latter is understandable because As is larger than P.

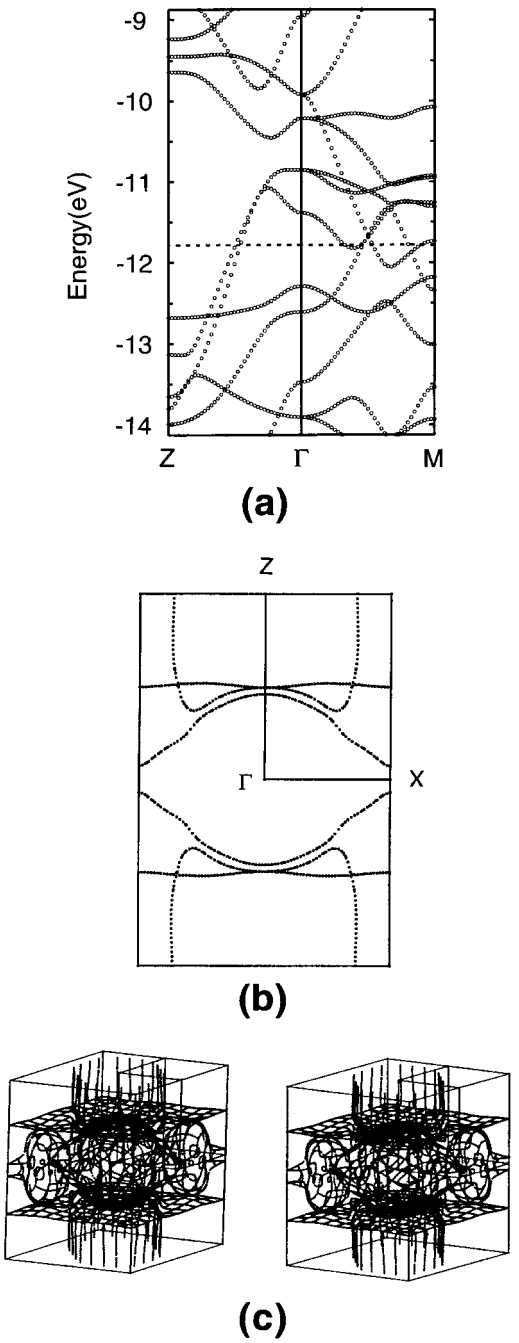

Figure 5. (a) Dispersion relations of the bands in the vicinity of the Fermi level calculated for h-ZrRuP, where the dashed line refers to the Fermi level. (b) Cross-section view of the Fermi surfaces of h-ZrRuP on the YZ plane. (c) Perspective stereoview of the Fermi surfaces of h-ZrRuP. Γ = (0, 0, 0), Y = (0, $^1/_2$, 0), Z = (0, 0, $^1/_2$) and M = ($^1/_2$, $^1/_2$, 0).

(21) Whangbo, M.-H.; Seo, D.-K.; Canadell, E. In *Physics and Chemistry of Low-Dimensional Inorganic Conductors*; Schlenker, C., Dumas, J., Greenblatt, M., van Smaalen, S., Eds.; Plenum: New York, 1996; p 285.

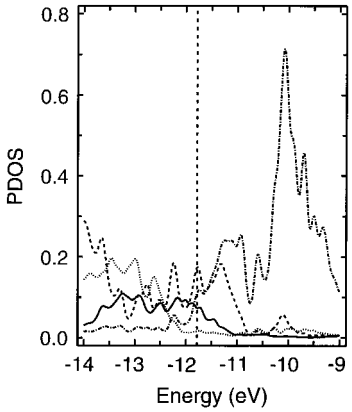

Figure 6. PDOS plots calculated for the $3p_z$ orbital of P and the $4d_{z^2}$ orbitals of Ru and Zr, where the solid line refers to P(1), the dotted line to P(2), the dashed line to Ru, and the dashed−dotted line to Zr. For simplicity of comparison, the PDOS value was normalized to one atom in each group of equivalent atoms.

h-ZrRuSi and h-ZrRuP are isostructural, and h-ZrRuSi has one less valence electron than does h-ZrRuP. Therefore, the electronic structures of the two compounds would be similar, in particular, showing the presence of a partially filled 1D band dispersive along the *c* direction. Figure 7a shows dispersion relations of the bands of h-ZrRuSi in the region of the Fermi level. The Fermi surfaces associated with the partially filled bands of Figure 7a are presented in Figure 7b as a cross-section view of the YZ-plane and in Figure 7c as a perspective stereoview. The Fermi surfaces of h-ZrRuSi are more complex than those of h-ZrRuP. Nevertheless, h-ZrRuSi possesses a pair of warped 1D Fermi surface sheets as does h-ZrRuP. From Figure 7a,b it is clear that the 1D band is less than half-filled.

In structures and atom compositions forming their prismatic chains, o-ZrRuP and h-ZrRuP are considerably different. Thus, the partially filled bands of o-ZrRuP may differ substantially from those of h-ZrRuP. Figure 8a shows dispersion relations of the bands of o-ZrRuP in the region of the Fermi level. The Fermi surfaces associated with the partially filled bands of Figure 8a are presented in Figure 8b as cross-section views of the *XZ* and *YZ* planes and in Figure 8c as a stereoview. These Fermi surfaces do not possess a 1D Fermi surface, in sharp contrast to the case of h-ZrRuP. The consequence of this difference between h-ZrRuP and o-ZrRuP is discussed in the next section.

5. Trends in the Superconducting Transition Temperatures

The Ru−Ru distance is shorter in h-ZrRuP than in elemental Ru metal (2.63 versus 2.68 Å). Barz et al.[1] speculated that the Ru−Ru bond contraction is important for the superconductivity of h-ZrRuP. As shown experimentally,[7−9] however, the T_c of the h-TRuX phase is not sensitive to the Ru−Ru distance. Figure 2b shows that the overlap population of the Ru−Ru bond in h-ZrRuP is not large. This is so because the Ru d orbitals are almost completely filled due to the electron transfer from the high-lying d orbitals of Zr. The change in Ru−Ru distance should not significantly affect the transport properties of h-TT'X, since the Ru d-orbital character is not strong near the Fermi level.

As found experimentally and calculated in the present work, the $N(E_f)$ values for h-ZrRuP and o-ZrRuP are small [0.21 and 0.29 state/(eV·atom), respectively, from our calculations]. Therefore, the higher T_c of h-ZrRuP compared that of o-ZrRuP (13.0 and 3.5 K, respectively) cannot be explained in terms of $N(E_f)$ values. According to the BCS theory, the T_c is related to the electron−phonon coupling constant λ and the Debye

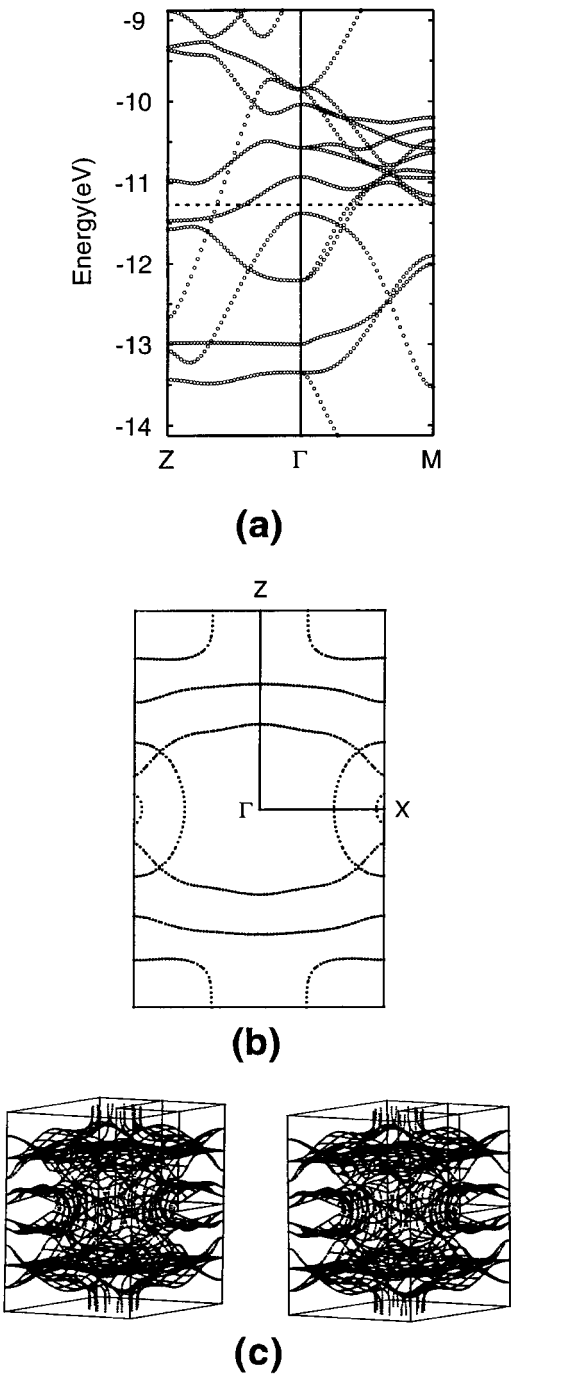

Figure 7. (a) Dispersion relations of the bands in the vicinity of the Fermi level calculated for h-ZrRuSi, where the dashed line refers to the Fermi level. (b) Cross-section view of the Fermi surfaces of h-ZrRuSi on the YZ plane. (c) Perspective stereoview of the Fermi surfaces of h-ZrRuSi. Γ = (0, 0, 0), Y = (0, $^1/_2$, 0), Z = (0, 0, $^1/_2$), and M = ($^1/_2$, $^1/_2$, 0).

temperature Θ_D as follows:[10,11]

$$T_c = \frac{\Theta_D}{1.45} \exp\left[- \frac{1.04(1+\lambda)}{\lambda - \mu^*\left(1 + \lambda\frac{\langle\omega\rangle}{\omega_0}\right)} \right] \qquad (1)$$

where the Coulomb pseudopotential $\mu^* \approx 0.1$ and the frequency ratio $\langle\omega\rangle/\omega_0 \approx 0.5$. In terms of Θ_D alone, T_c is predicted to be lower for h-ZrRuP than for o-ZrRuP (Θ_D = 345 and 454 K for h-ZrRuP and o-ZrRuP, respectively), in disagreement with experiment. Thus the electron−phonon coupling constant λ is important in making T_c higher for h-ZrRuP than for o-ZrRuP (13.0 and 3.5 K, respectively). For from eq 1 the λ values of

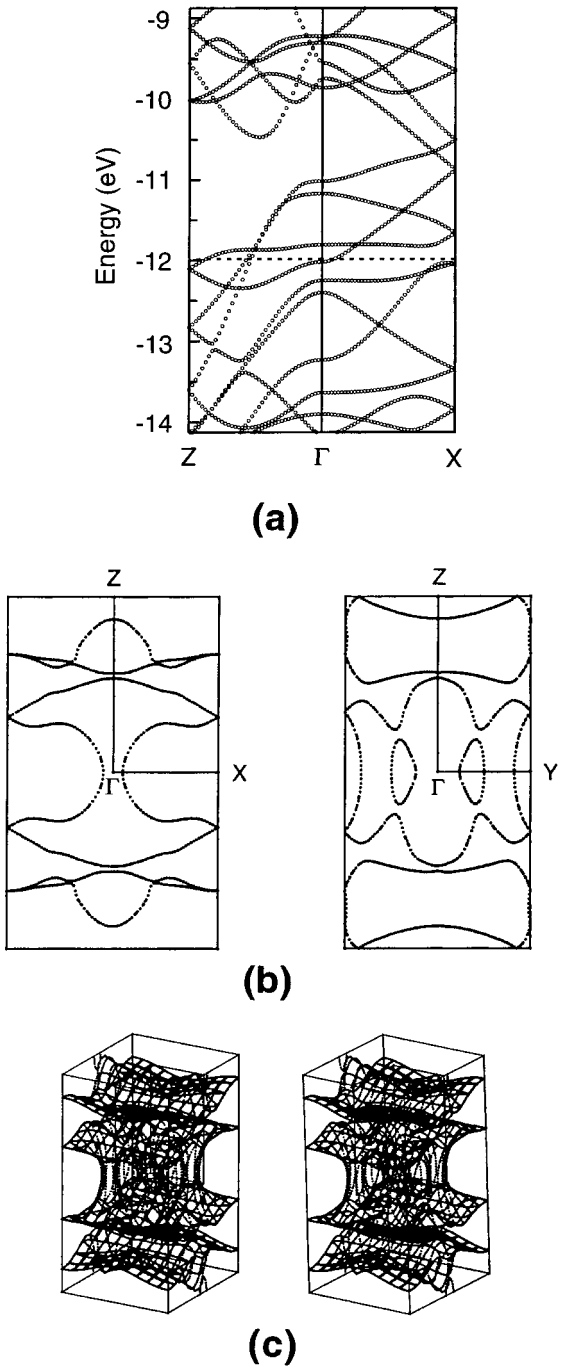

Figure 8. (a) Dispersion relations of the bands in the vicinity of the Fermi level calculated for o-ZrRuP, where the dashed line refers to the Fermi level. (b) Cross-section views of the Fermi surfaces of o-ZrRuP on the XZ and YZ planes. (c) Perspective stereoview of the Fermi surfaces of o-ZrRuP. Γ = (0, 0, 0), X = ($^1/_2$, 0, 0), Y = (0, $^1/_2$, 0), and M = ($^1/_2$, $^1/_2$, 0).

h-ZrRuP and o-ZrRuP are calculated to be 0.77 and 0.46, respectively, using their observed T_c and Θ_D.[8]

To examine why h-ZrRuP has a substantially larger λ value than does o-ZrRuP, we note that, for a lattice of atoms with mass M, the coupling constant λ is written as

$$\lambda = \frac{N(E_f)\langle I^2\rangle}{M\langle\omega^2\rangle} \qquad (2)$$

where $\langle I^2\rangle$ is the square of the electron−phonon matrix element averaged over the Fermi surface and $\langle\omega^2\rangle$ is the square of the phonon frequencies over the phonon band. Our calculations show that h-ZrRuP and o-ZrRuP have similar $N(E_f)$ values. Thus, provided that the two phases have similar $\langle I^2\rangle$ values, the difference in their λ values results from the difference in their $1/M\langle\omega^2\rangle$ values. The $M\langle\omega^2\rangle$ term has the dimension of a force constant, so that a large λ results when the lattice has soft phonons. That is, when the lattice is soft toward the low-frequency phonons crucial for superconductivity, the electron−phonon coupling constant λ is large, thereby raising the T_c.[22,23] This suggests that h-ZrRuP has softer phonons than does o-ZrRuP.

As discussed in the previous section, an important difference between h-ZrRuP and o-ZrRuP is that h-ZrRuP has a partially filled 1D band, while o-ZrRuP does not. A CDW instability associated with this band may not be strong enough to induce a *c*-axis doubling distortion in h-ZrRuP, but it may help create soft phonons conducive for superconductivity, thereby leading to its large T_c value. This explanation should also be applicable to why the T_c of h-ZrRuSi is much higher than that for o-ZrRuSi.

From the observation of superconductivity in h-TT′X and no superconductivity in o′-TT′X, it was pointed out[5] that undistorted −T−T′− zigzag chains are important for superconductivity. Superconductivity is absent in o′-HfRuAs and o′-TiRuAs probably because the *c*-axis doubling distortion removes soft phonons conducive to the formation of a superconducting state. Such a competition between CDW and superconductivity has also been observed for hexagonal alkali-metal tungsten bronzes A_xWO_3 (A = K, Rb, Cs).[24−27] The Fermi surfaces of these bronzes include a 1D Fermi surface, which causes a CDW transition in K_xWO_3 and Rb_xWO_3 but not in Cs_xWO_3. The x dependence of T_c and a CDW behavior of A_xWO_3 suggest that a CDW transition removes lattice phonons conducive to superconductivity.[24]

6. Concluding Remarks

To a first approximation, the electronic structures of h-ZrRuP and o-ZrRuP can be described from the viewpoint of the oxidation state $Zr^{4+}(RuP)^{4-}$. This picture leads to simple explanations for the low $N(E_f)$ values of both h-ZrRuP and o-ZrRuP, why h-ZrRuP has a nearly half-filled 1D band dispersive along the *c* direction, and why this band is largely associated with the $P(2)Ru_3$ prismatic chains. A CDW instability associated with such a 1D band is a likely cause for the occurrence of the h-TT′X to o′-TT′X transition in HfRuAs and TiRuAs phases. h-ZrRuP does not undergo an h-TT′X to o′-TT′X distortion probably because the CDW instability is not strong enough. Nevertheless, this instability appears to provide soft phonons conducive to superconductivity, thereby leading to a high T_c for h-ZrRuP. This view is consistent with the observation that o-ZrRuP does not possess a partially filled 1D band and its T_c is low. The absence of superconductivity in the o′-TT′X phases suggests that the CDW formation removes the phonons conducive to superconductivity.

Acknowledgment. Work at North Carolina State University was supported by the U.S. Department of Energy, Office of Basic Sciences, Division of Materials Sciences, under Grant DE-FG05-86ER45259, and by NATO, under Grant CRG 910129, Scientific Affairs Division.

IC970148S

(22) Whangbo, M.-H.; Williams, J. M.; Schultz, A. J.; Emge, T. J.; Beno, M. A. *J. Am. Chem. Soc*. **1987**, *109*, 90.
(23) Williams, J. M.; Ferraro, J. R.; Thorn, R. J.; Carlson, K. D.; Geiser, U.; Wang, H. H.; Kini, A. M.; Whangbo, M.-H. *Organic Superconductors*; Prentice Hall: New York, 1992.
(24) Lee, K.-S.; Seo, D.-K.; Whangbo, M.-H. *J. Am. Chem. Soc*. **1997**, *119*, 4043.
(25) Stanley, R. K.; Morris, R. C.; Moulton, W. G. *Phys. Rev*. **1979**, *B20*, 1903.
(26) Skokan, M. R.; Moulton, W. G.; Morris, R. C. *Phys. Rev*. **1979**, *B20*, 3670.
(27) Cadwell, L. H.; Morris, R. C.; Moulton, W. G. *Phys. Rev*. **1981**, *B23*, 2219.